

Yumen conglomerate ages in the South Ningxia Basin, north-eastern Tibetan Plateau, as constrained by cosmogenic dating

Wei Shi^{1,2} | Jianmin Hu¹ | Peng Chen^{1,3} | Hong Chen¹ | Yongchao Wang¹ | Xiang Qin¹ | Yu Zhang¹ | Yong Yang¹

¹Institute of Geomechanics, Chinese Academy of Geological Sciences, Beijing, China

²Key Laboratory of Neotectonic Movement and Geohazard, Ministry of Natural Resources, Beijing, China

³Department of Geophysics, Graduate School of Science, Kyoto University, Kyoto, Japan

Correspondence

Wei Shi, Institute of Geomechanics, Chinese Academy of Geological Sciences, Beijing 100081, China.

Email: shiweimg@163.com

Funding information

China Geological Survey (CGS), Grant/Award Number: DD20160060 and 1212011120100; National Natural Science Foundation of China, Grant/Award Number: 41672203; Basic Research Operating expenses Program, Grant/Award Number: DZLXJK201712

Handling Editor: S. Li

The South Ningxia Basin, as the outermost Cenozoic basin on the north-eastern margin of the Tibetan Plateau, is characterized by a series of convex to the north-east arcuate structural belts. Constraining the final formation time of the belt has been an ongoing focus in geologic research of the Tibetan Plateau. A set of early Pleistocene conglomerates, the Yumen conglomerate, overlying the folded pre-Quaternary formations are widely distributed throughout the whole basin, and the latest folded formation is the upper Pliocene Ganhegou Formation, marking the termination of folding uplift in the north-eastern Tibetan Plateau. Based on 1:50,000 geological mapping, a set of early Pleistocene alluvial fan conglomerates overlying the folded Palaeogene–Neogene strata were recognized and agree well with the Yumen conglomerate. Here, the Yumen conglomerate formation ages were determined to be 0.6–1.04 Ma using cosmic nuclide burial dating. Combined with the upper limit age of the latest strata beneath the unconformity with the latest palaeomagnetic age of 2.77 Ma, the crustal shortening event is restricted to the period 2.77–1.04 Ma, indicating that it is the most intense tectonic shortening event along the north-eastern margin of the Tibetan Plateau.

KEYWORDS

cosmogenic nuclide burial dating, north-eastern Tibetan Plateau, orogeny, Pleistocene, South Ningxia Basin, Yumen conglomerate

1 | INTRODUCTION

The north-eastern margin of the Tibetan Plateau records tectonic information regarding the north-eastward expansion of the Tibetan Plateau (Figure 1; RGAFSO, 1988; Shi et al., 2015). This area in terms of geometry is characterized by convex to the north-east arcuate structural belts resulting from the blockage of the northern Alxa Massif and the eastern Ordos Massif. The topographic morphology is characterized by a basin-and-range structure including the Haiyuan–Xingrenpu, Tongxin, and Hongsipu basins and the Yueliangshan–Nanhuashan–Huangjiawashan, Xiangshan–Tianjingshan, Yantongshan, and Luoshan–Niushoushan mountains (Figure 1; RGAFSO, 1988; Zhang et al., 1990). At the leading edges of each basin-and-range

structure, the Haiyuan (F_1), Xiangshan–Tianjingshan (F_2), Yantongshan (F_3), and Niushoushan–Luoshan fault zones (F_4) are successively aligned from south-west to north-east (Figure 1; Shi et al., 2015). Numerous studies have shown that Pleistocene conglomerates overlying Palaeogene–Neogene strata in an angular unconformity are widely distributed along the north-eastern margin of the Tibetan Plateau (Shi et al., 2015), reflecting a major tectonic event resulting in the formation of a topographic framework (Burchfiel et al., 1991; Chen et al., 2015; Duvall et al., 2013; RGAFSO, 1988; Shi et al., 2013, 2015; Zhang et al., 1990). Based on regional tectonic analysis, the deformation age of this tectonic event was approximately ascertained as late Pliocene–early Quaternary (Shi et al., 2015; Zhang et al., 1990). Reliable evidence to accurately restrict the age of this tectonic event

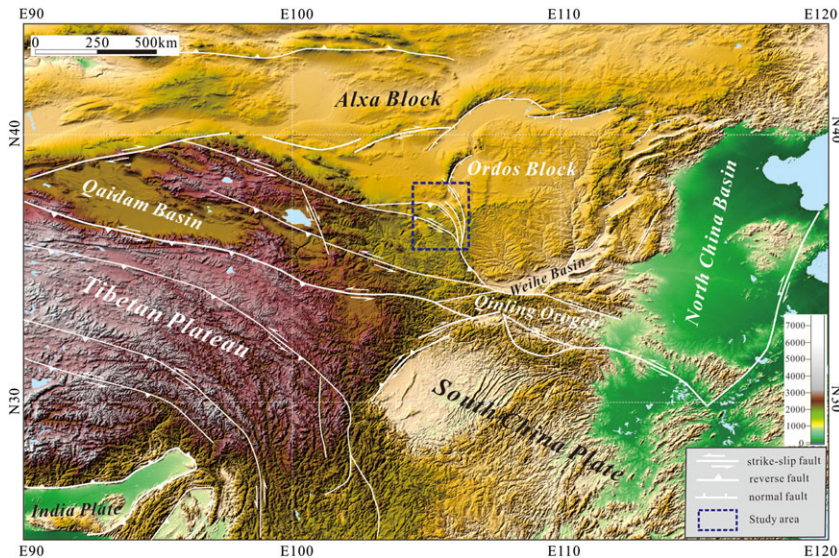


FIGURE 1 Structural outline of Central North China and the location of study area based on digital elevation model (DEM; DEM from <https://wist.echo.nasa.gov/wist-bin/api/ims.cgi?mode=MAINSRCH&JS=1>) [Colour figure can be viewed at wileyonlinelibrary.com]

remains lacking. Recently, 1:50,000 geological mapping in the South Ningxia Basin was conducted to uncover a set of early Pleistocene conglomerates, the Yumen conglomerate, along the north-eastern margin of the Tibetan Plateau (Shi, Chen, Li, Gong, & Qiu, 2016). The Yumen conglomerate typically are developed with near-horizontal bedding structures and overlay the pre-Quaternary folded strata in an angular unconformity. Cosmological nuclide dating has been widely applied for direct dating of geomorphic surface ages of Pliocene or younger age during the recent two decades (Gosse & Phillips, 2001); here, this technique was used to determine the burial age of the lower Pleistocene conglomerates in the north-eastern Tibetan Plateau, helping to constrain the accurate deformation age of this tectonic event.

2 | GEOLOGICAL SETTING

The Haiyuan Fault zone extends from Xiaokou at the eastern piedmont of Liupanshan Mountain north-westward through the Yueliangshan, Nanhuashan, Xihuashan, Huangjiawashan, Hasishan, and Halashan mountains before terminating in Jingtai County, Gansu Province. It has a total length of approximately 200 km, forming the most significant fault zone along the north-eastern margin of the Tibetan Plateau (Figure 2; IG & SBNHAP, 1990). The Haiyuan Fault is a left-lateral strike-slip fault with strong seismicity during the Quaternary (Burchfiel et al., 1991; Shi et al., 2015). Geophysical data show that the fault zone is a significant gravity anomaly gradient zone and the lithosphere dramatically thins along its deformational belt (Ye et al., 2015). The fault zone is mainly developed along the sides of the striped-shape uplifted ranges and is spliced by en echelon secondary faults and small-scale pull-apart basins bounded by these secondary faults (IG & SBNHAP, 1990). The approximately 150-km-long Xiangshan–Tianjingshan Fault zone can be divided into eastern and western segments with a right-steepening geometric pattern. The NW-trending

western segment extends along the northern piedmont of the Xiangshan and Tianjingshan mountains and connects with the Gulang and Lenglongling fault zones. The eastern segment changes from NW-trending to N–S-trending in the Hanjiaoshui–Heicheng–Guyuan area and may extend to the Liupanshan fault zone in the Guyuan area. The Yantongshan fault zone begins in Yashigou in Zhongwei County to the north and extends south-eastward through the Yellow River, the eastern piedmont of the Yantongshan and Yaoshan mountains, and the western piedmont of Tanshan, before disappearing southward under loess deposits. The approximately 590-km-long Niushoushan–Luoshan fault zone is the outermost boundary fault of the north-eastern margin of Tibetan Plateau and is bounded by the Tibetan Plateau, North China Block, and Alxa Block (Chen et al., 2015). The fault zone begins near Jingyuan County to the south, extends northward through the Yunwushan and Daluoshan mountains and the eastern piedmont of Xiaoluo Mountain, and then turns to the N–NW connecting with the north-eastern piedmont of Niushoushan Mountain and Yuanshanzi (Chen et al., 2015).

The Palaeogene and Neogene strata in this area consist of the Sikouzi, Qingshuiying, Zhangenpu, and Ganhegou formations (ECRGCN, 2017). Except for the micro-angle or parallel unconformity between the Ganhegou Formation and the Zhangenpu Formation, no significant angular unconformity has been observed among the other formations (BGMN, 1990; Liu et al., 2019). The Sikouzi Formation is largely characterized by fluvial-lacustrine sediments composed of brick red and purple-red medium-to-thick layered conglomerates, glutenite, and coarse sandstones. Red thick-bedded coarse sandstones feature large-scale interlaced and oblique bedding. This formation overlies the early Cretaceous Najiha Formation in a parallel unconformity (Shi et al., 2013). The Sikouzi Formation, hundreds of metres in thickness, is locally distributed on the eastern side of the Xiangshan–Tianjingshan Mountains and the northern side of Madongshan Mountain. Eocene fossils have been found in the Sikouzi Formation (RGSNX, 2000).

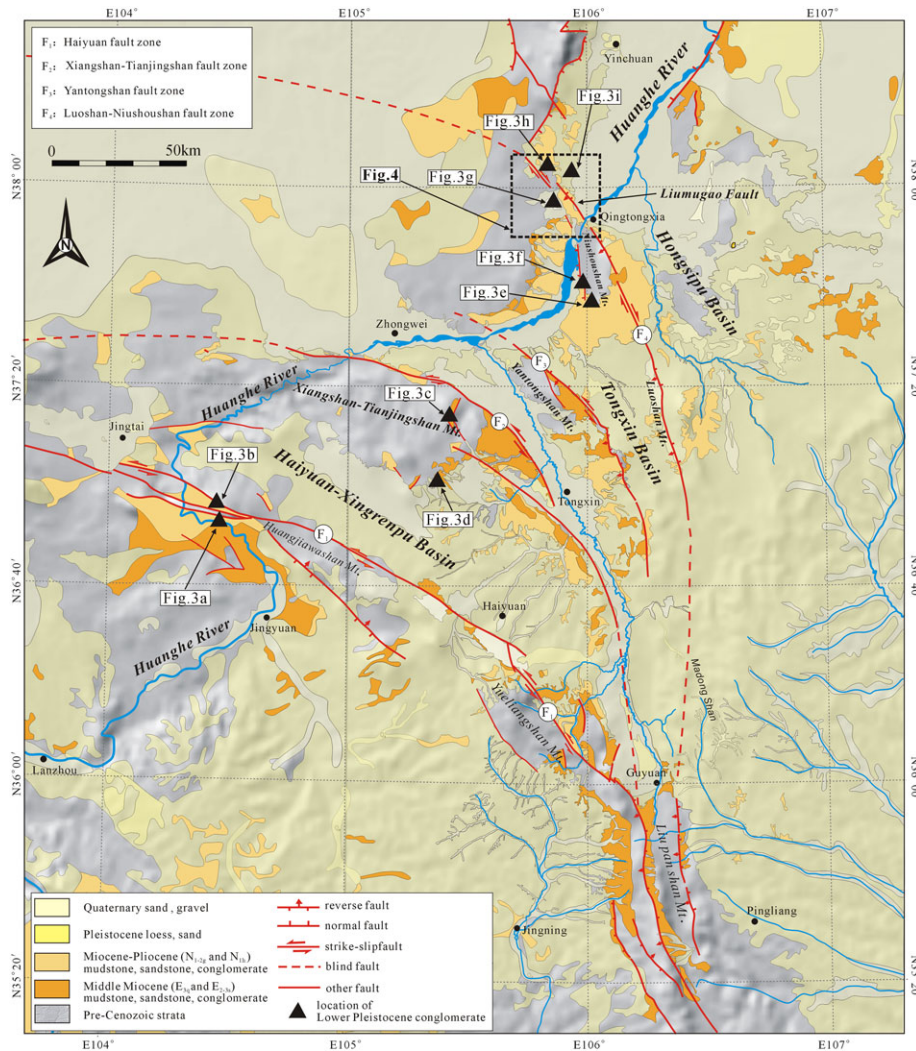


FIGURE 2 Schematic geological map of the north-east periphery of the Tibetan Plateau, showing the Cenozoic basins, boundary faults, and the locations for a regional angular unconformities between the Early Pleistocene Yumen conglomerate and the underlying stratigraphic rocks [Colour figure can be viewed at wileyonlinelibrary.com]

The lower part of the Qingshuiying Formation is composed of brownish-red sandstone, siltstone, and argillaceous siltstone with some red mudstone. Its upper part is characteristically brown-red, orange-red, and purple-red mudstone, grey-green mudstone-clad gypsum, and an argillaceous gypsum layer indicating a salt lacustrine sediment. The formation is marked by widely distributed gypsum more than 1,000 m thick. Early vertebrate fossils, sporopollen, and palaeomagnetic data indicate that the Qingshuiying Formation formed during the Oligocene (BGMN, 1990; Shen, Tian, Ding, Wei, & Chen, 2001). The Zhangenpu Formation is a typical deep lacustrine sediment with lithological assemblages of light red, orange-red, and orange-yellow mudstone, occasionally containing some gypsum. The formation is weakly consolidated with a lighter colour than that of the underlying Qingshuiying and Sikouzi formations (ECRGCN, 2017). Animal fossils together with gastropods, spirulina, and ostracods indicate it formed during the early and middle Miocene (Qiu & Ye, 1988; Wang, Yan, Lu, & Chen, 1994). The latest palaeomagnetic results show that the

sedimentary age of this formation is 23.8–9.7 Ma (Liu et al., 2019), in agreement with the fossil data.

The Ganhegou Formation is dominated by fluvial strata including yellowish-brown grey-white conglomerates, glutenite, and sandstones with poor cementation (Wang, Zhang, & Kirby, 2011). Palaeomagnetic results show an older age limit of ~9.5 Ma but possibly extending into the mid-late Pliocene (~2.58 Ma; Jiang, Ding, & Xiong, 2007; Lin, Chen, Wyrwoll, & Cheng, 2010; Liu et al., 2019). The sedimentary profile shows an obvious sedimentary discontinuity with the underlying Zhangengpu Formation (Liu et al., 2019; Shen et al., 2001). The early Pleistocene formation has a very limited distribution and lies unconformably over Palaeogene, Neogene, or Cretaceous strata (BGMN, 1990; Shi et al., 2015). The formation is mainly exposed along a piedmont river valley with well-consolidated light-purple or grey conglomerates at the bottom, thought to be Yumen conglomerate (BGMN, 1990). The upper part is a grey sand-gravel layer and is aged as lower Pleistocene from vertebrate fossils contained in the conglomerates.

3 | SPATIAL DISTRIBUTION AND SEDIMENTARY FEATURES OF THE YUMEN CONGLOMERATE

A group of early Pleistocene conglomerates is widely distributed at the top or highlands of hills and in valleys with a sub-horizontal bedding structure in the South Ningxia Basin, along the north-eastern periphery of the Tibetan Plateau. Together with underlying stratigraphic rocks, it forms regional angular unconformities in this region (Figures 2 and 3; Shi et al., 2015). This stratum is identified as lower Pleistocene Yumen conglomerate in the Ningxia regional geological survey based on lithology, sedimentary facies, occurrence, and comparison to regional strata (BGMN, 1990).

In the interior of the Haiyuan Fault, the innermost part of the South Ningxia Basin, these early Pleistocene Yumen conglomerate cover folded early Pliocene conglomerates (Figure 3a). North-west-striking thrusts and early Pliocene conglomerates along the major Haiyuan Fault are overlapped by the early Pleistocene Yumen conglomerate, suggesting a NE-SW shortening prior to the early Pleistocene (Figure 3b; Shi et al., 2015). Our structural investigation shows a regional angular unconformity for the Yumen conglomerate and overlying Oligocene sandstone, a conglomerate (Qingshuiying Formation) in the interior of Tianjingshan Mountain (Figure 3c) and Yumen conglomerate unconformably in contact with Eocene conglomerate (Sikouzi Fm.) along the southern periphery of Tianjingshan Mountain (Figure 3d). Along the west margin of Niushoushan Mountain, the Yumen conglomerate cover Early Miocene mudstone (N_{1z}), and Oligocene mudstone (E_{3q}), dominating a regional angular unconformity (Figure 3e,f). The Yumen conglomerate also unconformably overlies the Oligocene mudstone (E_{3q}) south-west of the Liumugao Fault (Figure 3g), the Early Miocene mudstone (N_{1z}) north-east of the Liumugao Fault (Figure 3h), and a Late Miocene-Pliocene conglomerate (N_{1-2g} ; Figure 3i).

Geological mapping at a 1:50,000 scale along the northern segment of the Luoshan-Niushoushan Fault zone was conducted, and the distribution and stratigraphic characteristics of the Yumen conglomerate were recognized along the Liumugao Fault in the outermost periphery of the Tibetan Plateau which belongs to the north segment of the Luoshan-Niushoushan Fault zone (Figures 4 and 5; Shi et al., 2016). The Yumen conglomerate are mainly distributed at the frontal edge of the central Liumugao Fault with a fan-shaped distributional pattern and overlie the Ganhegou Formation and other older strata (Figures 3-5). The thickness of the conglomerates varies from ~1 to 6 m, with a gradient thinning from the piedmont area to the Yinchuan Basin. The detailed large-scale geological survey shows that the conglomerates are a group of alluvial coarse-grain clastic rocks composed of a grey-brownish grey thick layer of blocky calcareous medium- and coarse-grained conglomerates sandwiched with yellow silty sandstones or lens bodies. The particle size of the gravels is approximately 1-6 cm with poor roundness and cemented by sandy, muddy, and calcium cementation (Figure 5). From the piedmont to the basin, the particle size gradually decreases. The gravels contained in the conglomerates show complex assemblages with dominant sandstone and limestone and limited metamorphic rock, granite,

and quartz. The source area of the Yumen conglomerate was traced to the west-south-west side of the mapping area according to palaeocurrent data, indicating that the source materials are from Jurassic sandstone and conglomerates and Cambrian-Ordovician limestone, a typical alluvial origin determined from the sedimentary characteristics (Figure 5).

4 | THE DATING OF THE YUMEN CONGLOMERATES

Previous studies show the cosmological nuclide dating is one of most effective methods to directly dating Quaternary conglomerates (Çiner et al., 2015; Sarikaya, Çiner, & Zreda, 2015). Here, we use this technique to determine the burial ages of the Pleistocene conglomerates.

4.1 | Sample collection

Sample collection was carried out at the conglomerates tableland with different altitudes and different strata from the underlying strata. To determine the burial age of the conglomerates, the bottom of the conglomerates were sampled, and pure quartz gravels were collected and then were used to test the burial age of cosmogenic nuclides. Here, a total of three samples were collected in the South Ningxia Basin, and at least 20 gravels were selected for each sample, with a total weight of 500 g or more (Table 1).

Accelerator mass spectrometry (AMS) measurement errors are at 1 s level, including statistical (counting) error and error due to normalization of standards and blanks. The error weighted average $^{10}\text{Be}/^9\text{Be}$ full-process blank ratio is $(3.13 \pm 0.36) \times 10^{-15}$. $^{26}\text{Al}/^{10}\text{Be}$ ratios are calculated with the CRONUS-Earth exposure age calculator and are referenced to Balco et al. (2009).

4.2 | Sample pretreatment and testing

The sample processing and testing were completed at the Xi'an Accelerator Mass Spectrometry Center of Xi'an Loess Institute of Chinese Academy of Sciences. Sample pretreatment mainly removes impurities from the sample in the laboratory to purify the quartz. The process was as follows: the sample was washed with water to remove the clay; the sample was heated in 3 mol/L HCl for 6 hr to remove the limestone in the sample; the sample was immersed in a 1% HF + 1% HNO_3 solution and heated to 80°C; and the sample was subjected to ultrasonic disturbance for 8-12 hr; the solution was replaced several times to obtain pure quartz.

Sample testing included the determination of the Be and Al contents, as well as the $^{10}\text{Be}/^9\text{Be}$ ratio and the $^{26}\text{Al}/^{27}\text{Al}$ ratio. First, pure quartz was weighed, and 0.5235 mg of ^9Be carrier was added. The quartz was dissolved in HF, and part of the solution was removed and diluted to determine the Al content in the quartz. The remaining solution was extracted with an anion resin, acetylaceton-carbon tetrachloride, and a cationic resin to finally obtain the Be and Al components. Then, the Be and Al components were converted to $\text{Be}(\text{OH})_2$ and $\text{Al}(\text{OH})_3$ with ammonia water and were precipitated, and then



FIGURE 3 Field photographs of the regional angular unconformities between the Early Pleistocene Yumen conglomerates and the underlying stratigraphic rocks in the north-east periphery of the Tibetan Plateau. (a) The regional angular unconformity composed of the Early Pleistocene Yumen conglomerates and the folded Early Pliocene sandstone in the interior of the Haiyuan Fault. (b) The Early Pleistocene Yumen conglomerate covering north-west-striking thrusts and Early Pliocene conglomerates along the major Haiyuan Fault (Shi et al., 2015). (c) The regional angular unconformity between the Yumen conglomerate and Oligocene sandstone, conglomerate (Qingshuiying Fm.) in the interior of the Tianjingshan Mt. (d) The Yumen conglomerate unconformably overlying Eocene conglomerate (Sikouzi Fm.) in the south periphery of the Tianjingshan Mt. (e, f) The regional angular unconformities between the Yumen conglomerate and the Early Miocene mudstone (N₁₂), and Oligocene mudstone (E_{3q}) in the west margin of the Niushoushan Mt., respectively. (g) The Yumen conglomerate unconformably overlying the Oligocene mudstone (E_{3q}) in the south-west of the Liugugao Fault, and on the Early Miocene mudstone (N₁₂) in the north-east of the Liugugao Fault (h). (i) Yumen conglomerate unconformably covering Late Miocene–Pliocene conglomerate and sandstone (N_{1–2g}) [Colour figure can be viewed at wileyonlinelibrary.com]

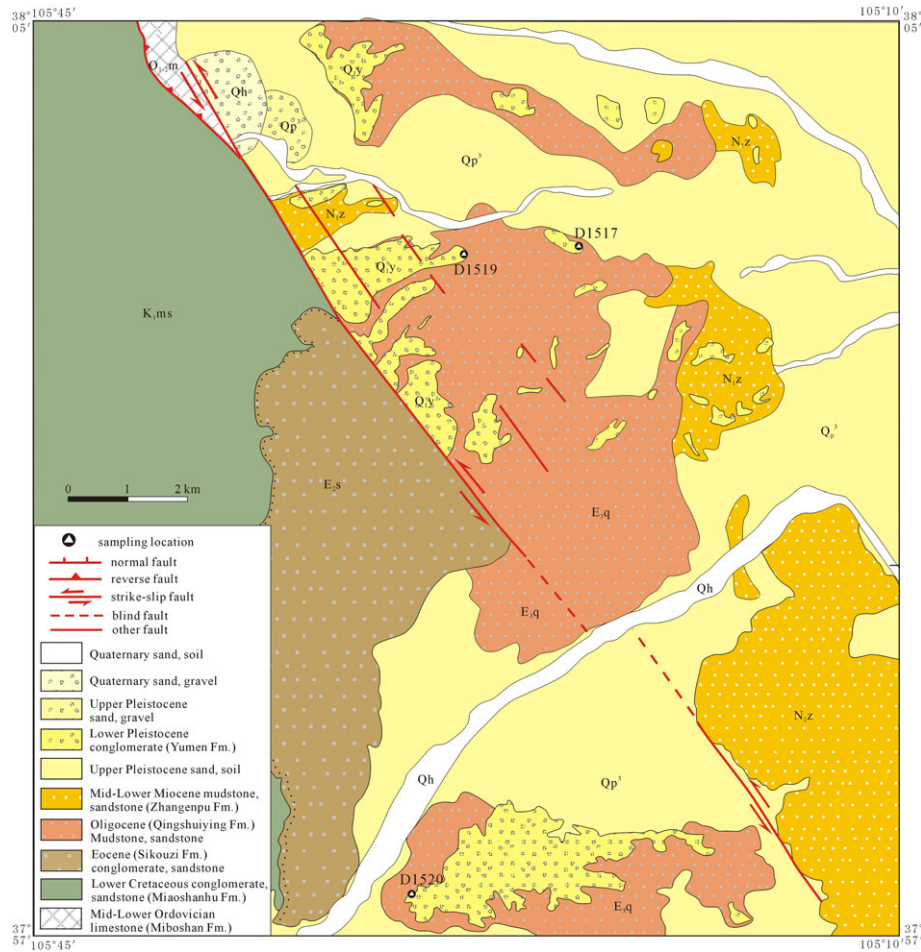


FIGURE 4 Geological map of the Liumugao Fault, the northeasternmost Tibetan Plateau and sampling locations [Colour figure can be viewed at wileyonlinelibrary.com]

Be(OH)₂ and Al(OH)₃ were heated in a muffle furnace at 950°C for 1 hr to form BeO and Al₂O₃; BeO and Al₂O₃ were mixed with high-purity Nb powder and Ag powder, respectively, to form a target, and were finally placed in an accelerator mass spectrometer (AMS) to determine the ratio of ¹⁰Be/⁹Be and ²⁶Al/²⁷Al (Sharma et al., 2000). The AMS assay was performed at the Purdue University Accelerator Mass Spectrometry Center in the United States.

4.3 | Analysis of experimental data

The cosmogenic nuclide burial age method is based on the cosmic ray bombardment of rocks during the near-surface exposure to form cosmogenic nuclides. These surface rocks containing cosmogenic nuclides are denuded, transported and deposited, and covered by sediments. The content of the cosmogenic nuclides ¹⁰Be and ²⁶Al decay with the increase of burial time, and the ²⁶Al/¹⁰Be ratio also decreases with time. Thus, the rock deposition time can be calculated in terms of content and ratio of cosmogenic nuclide pairs in rocks, and the formulae can be used as follows (Granger & Muzikar, 2001):

$$N_{\text{Be}}(t) = P_{\text{Be}} e^{-\lambda_{\text{Be}} t / (\lambda_{\text{Be}} + \epsilon/L)} + N_{\text{Be}}(d), \quad (1)$$

$$N_{\text{Al}}(t) = P_{\text{Al}} e^{-\lambda_{\text{Al}} t / (\lambda_{\text{Al}} + \epsilon/L)} + N_{\text{Al}}(d), \quad (2)$$

where $N_{\text{Be}}(t)$ and $N_{\text{Al}}(t)$ present the contents of ¹⁰Be/²⁶Al with the burial time interval of quartz, respectively; λ_{Be} and λ_{Al} express decay constant for ¹⁰Be and ²⁶Al nuclides, respectively; P_{Be} and P_{Al} are rates of ¹⁰Be/²⁶Al nuclide concentrations, respectively; L is decay length of cosmic-ray particle (160/(ρ cm)); ρ is density of the overlying deposits of quartz. $N_{\text{Be}}(d)$ and $N_{\text{Al}}(d)$ are the contents of ¹⁰Be/²⁶Al nuclide posterior to burial quartz.

Here, the burial ages of three conglomerates were obtained in terms of the previously methods (Table 2).

5 | DISCUSSION

Increasingly, more studies have shown that strong NE-SW-trending crustal shortening that occurred in the north-eastern margin of the Tibetan Plateau is constrained to the late Pliocene–early Quaternary and resulted in the formation of the arcuate structural belts (Burchfiel et al., 1991; RGAFSO, 1988; Shi et al., 2013, 2015; Zhang et al., 1990, 1991; Zhang & Cai, 2006; Zhang, Liao, Shi, & Hu, 2006). These belts comprise the basic geomorphic pattern of the north-eastern margin

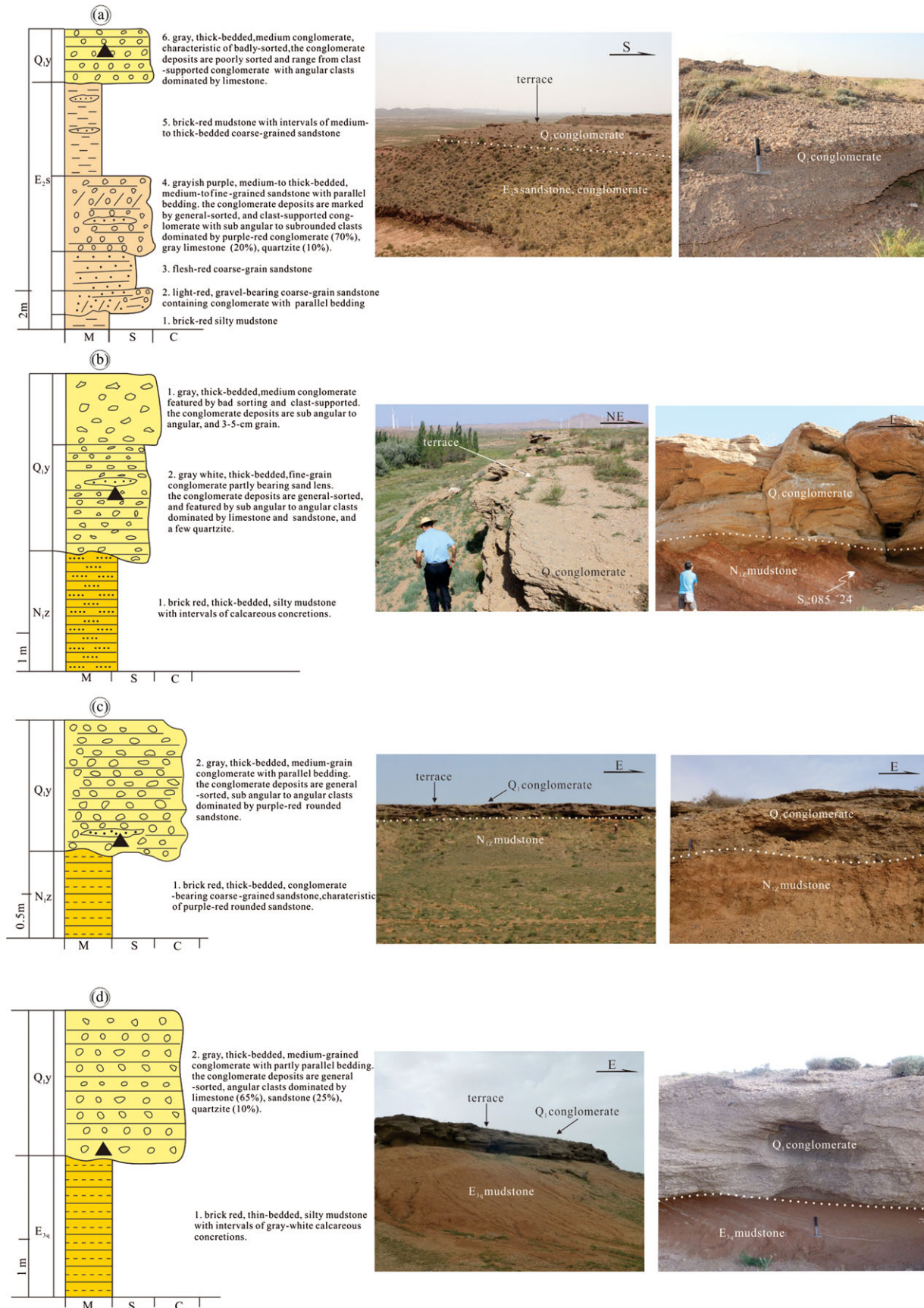


FIGURE 5 Stratigraphic sections of the regional angular unconformities between the Early Pleistocene Yumen conglomerate and the underlying pre-Quaternary strata along the Liumugao Fault, and the locations of the cosmogenic nuclide samples [Colour figure can be viewed at wileyonlinelibrary.com]

TABLE 1 AMS $^{26}\text{Al}/^{27}\text{Al}$ and $^{10}\text{Be}/^9\text{Be}$ results of the samples from the South Ningxia Basin

Sample code	Longitude/latitude	Sample weight (g)	$^{10}\text{Be}/^9\text{Be}$ ratio	Uncertainty (%)	^9Be weight (mg)	$^{26}\text{Al}/^{27}\text{Al}$ ratio	Uncertainty (%)	^{27}Al weight (mg)	$^{26}\text{Al}/^{10}\text{Be}$
D1517	38°02'57"105°51'15"	30.0004	8.71E-13	3.55	0.3260	1.82E-12	2.11	2.4735	15.84
D1519	38°03'55"105°49'56"	30.0186	9.22E-13	2.82	0.3319	2.08E-12	1.91	2.3877	16.20
D1520	37°57'02"105°49'12"	30.0273	3.81E-13	4.12	0.3328	3.99E-13	4.98	3.2300	10.17

TABLE 2 Burial Ages of samples from the South Ningxia Basin

Sample code	S	^{26}Al	^{26}Al err	^{10}Be	^{10}Be err	Burial Age (ka)	1 sigma	Erosion rate (cm/ka)	1 sigma
D1517	2.4620	3343981.8366	70560.0750	633208.0984	224575.7694	170.0	323.1	1.174	0.317
D1519	2.5432	3684232.6002	70357.9725	682405.8433	192628.6469	126.3	280.6	1.144	0.276
D1520	2.6353	957799.0542	47711.3693	282534.1073	116515.1021	1043.9	533.4	1.915	0.813

of the Tibetan Plateau and reflect the most intense tectonic deformation caused by the north-eastward expansion of the plateau (Shi et al., 2015). Here, based on 1:50,000 geological mapping of the north-eastern margin of the Tibetan Plateau, integrating high-precision magnetic stratigraphic chronology of the Palaeogene–Neogene in the basin (Liu et al., 2019), and cosmological dating of the Yumen conglomerate, the most intense tectonic deformation which caused the widespread folding uplift occurred on the north-eastern Tibetan Plateau (Shi et al., 2015) was restricted to the age span of ~2.77 to ~1.04 Ma. The cosmic nuclide dating result on the highest terrace in the Xiangshan–Tianjingshan fault zone was reported to be 2.4 Ma, which might represent the transformation age from thrusting to left-lateral strike-slip faulting (Zhang & Cai, 2006), consistent with the aforementioned result. The palaeochannel reconstruction along the north margin of the Qinling shows that the tributaries along its north margin have a higher incision of 144 ± 25 m since the late Early Pleistocene (~1.4–1.2 Ma), leading to the break-up of the Tianshui ancient lake (Shi et al., 2018), which also dominates the intensive north-eastward expansion of the Tibetan Plateau.

In fact, the traditional Yumen conglomerate are a piedmont molasse melange that developed in the Hexi Corridor (Fang et al., 2004; Huang et al., 1947; Wang, Wan, & Liu, 2003). Palaeomagnetic dating analysis showed that the sedimentary ages of these strata are 5–1.7 Ma and termed the Xiyu conglomerate in the Hexi Corridor (Qiao, Huang, Biggin, & Piper, 2017; Zhao et al., 2017). The conglomerates, occurring in the Tianshan area to the west of the Hexi Corridor, were determined to be 2.5–2.9 Ma in age based on palaeomagnetic dating and vertebrate fossil analysis (Chen, Lin, Guan, & Xu, 1994; Li et al., 2001; Peng, 1975; Qiao et al., 2017), also supporting that the northern margin of the Tibetan Plateau underwent a rapid uplift during the late-early Quaternary with the typical molasse melange (Jin, Wang, Chen, & Ren, 2003; Sun, Zhu, & Bowler, 2004). Of course, other studies also have noted that the Xiyu Formation is diachronous with a deposition time of 3.5–1.8 Ma (Fang et al., 2004). Actually, there is an angular unconformity existing in the stratigraphic sequences of the Xiyu Formation; subsequent palaeomagnetic studies have reported palaeomagnetic ages of the conglomerates to be 2.88–

2.58 Ma (Fang et al., 2004; Liu et al., 2011). These studies also demonstrated that a quasi-simultaneous orogenic event occurred along the northern and north-eastern margin of the Tibetan Plateau during the late Pliocene–early Quaternary (2.5 Ma).

6 | CONCLUSIONS

1. The early Pleistocene Yumen conglomerate along the north-eastern margin of the Tibetan Plateau, predominately composed of alluvial–proluvial deposits, were deposited during the period 1.04–0.6 Ma, as defined by cosmic nuclide burial age dating.
2. The younger strata of the Yumen conglomerate via cosmic nuclide burial are ~1.04 Ma in age, and the upper strata of the underlying youngest stratigraphic rocks (Ganhegou Formation) have palaeomagnetic ages of ~2.77 Ma, delimiting the time span of a regional angular unconformity along the north-eastern periphery of the Tibetan Plateau, consisting of the Yumen conglomerates and the underlying pre-Pleistocene strata, which represents the most intensive expansion of the Tibetan Plateau.

ACKNOWLEDGEMENTS

This study was supported by research Grants from China Geological Survey (CGS; DD20160060 and 1212011120100), Basic Research Operating expenses Program (DZLXJK201712), and National Natural Science Foundation of China (41672203). We are very grateful to Editors Profs. Sanzhong Li, Gang Rao, and anonymous reviewers for their critical and constructive comments to improve the manuscript.

ORCID

Wei Shi  <https://orcid.org/0000-0003-1452-1555>

REFERENCES

- Balco, G., Briner, J., Finkel, R. C., Rayburn, J. A., Ridge, J. C., & Schaefer, J. M. (2009). Regional beryllium-10 production rate calibration for late-

- glacial northeastern North America. *Quaternary Geochronology*, 4(2), 93–107. <https://doi.org/10.1016/j.quageo.2008.09.001>
- Burchfiel, B. C., Zhang, P. Z., Wang, Y. P., Song, F. M., Deng, Q. D., Molnar, P., & Royden, L. (1991). Geology of the Haiyuan Fault zone, Ningxia-Hui Autonomous Region, China, and its relation to the evolution of the northeastern margin of the Tibetan Plateau. *Tectonics*, 10, 1091–1110. <https://doi.org/10.1029/90TC02685>
- Bureau of Geology and Mineral Resources of Ningxia Hui Autonomous Region (BGMN) (1990). *Regional geology of Ningxia Hui autonomous region* (pp. 1–522). Beijing: Geological Publishing House.
- Chen, H., Hu, J. M., Wu, G. L., Shi, W., Geng, Y. Y., & Qu, H. J. (2015). Apatite fission-track thermochronological constraints on the pattern of late Mesozoic-Cenozoic uplift and exhumation of the Qinling Orogen, central China. *Journal of Asian Earth Sciences*, 114(4), 649–673. <https://doi.org/10.1016/j.jseae.2014.10.004>
- Chen, H. H., Lin, X. L., Guan, G. N., & Xu, J. M. (1994). Early Pleistocene deposits and its lower boundary (Q/N) in Tianshan MT., Xinjiang region. *Quaternary Sciences*, 1, 38–47.
- Çiner, A., Dogan, U., Yıldırım, C., Akçar, N., Ivy-Ochs, S., Alfimov, V., ... Schlüchter, C. (2015). Quaternary uplift rates of the Central Anatolian Plateau, Turkey: Insights from cosmogenic isochron-burial nuclide dating of the Kızılırmak River terraces. *Quaternary Science Reviews*, 107, 81–97. <https://doi.org/10.1016/j.quascirev.2014.10.007>
- Duvall, A. R., Clark, M. K., Kirby, E., Farley, K. A., Craddock, W. H., Li, C. Y., & Yuan, D. Y. (2013). Low temperature thermochronometry along the Kunlun and Haiyuan faults, NE Tibetan Plateau: Evidence for kinematic change during late stage orogenesis. *Tectonics*, 32, 1190–1121. <https://doi.org/10.1002/tect.20072>
- Editorial Committee of the Regional Geology of China, Ningxia (ECRCN) (2017). *The regional geology of China, Ningxia* (pp. 1–916). Beijing: Geological Publishing House.
- Fang, X. M., Zhao, Z. J., Li, J. J., Yan, M. D., Pan, B. T., Song, C. H., & Dai, S. (2004). The Late Cenozoic magnetic strata of the Laojunmiao anticline on the northern margin of the Qilian Mountains and the northern uplift of the plateau. *Chinese Science (D)*, 34(2), 97–106.
- Gosse, J. C., & Phillips, F. M. (2001). Terrestrial cosmogenic nuclides: Theory and applications. *Quaternary Sciences Review*, 20, 1475–1560. [https://doi.org/10.1016/S0277-3791\(00\)00171-2](https://doi.org/10.1016/S0277-3791(00)00171-2)
- Granger, D. E., & Muzikar, P. F. (2001). Dating sediment burial with in situ-produced cosmogenic nuclides: Theory, techniques, and limitations. *Earth and Planetary Science Letters*, 188, 269–281. [https://doi.org/10.1016/S0012-821X\(01\)00309-0](https://doi.org/10.1016/S0012-821X(01)00309-0)
- Huang, T. K., Young, C. C., Cheng, Y. C., Chow, T. C., Bien, M. N., & Wang, W. P. (1947). Report on geological investigation of some oil-fields in Sinkiang. Geol. Mem. Ser.A21 (Natl. Geol. Surv. of China, Nanking, 118.
- Institute of Geology, State Seismological Bureau (IG), Seismological Bureau of Ningxia Hui Autonomous Province (SBNHAP) (1990). *Haiyuan active fault* (pp. 1–286). Beijing: Seismological Press.
- Jiang, H. C., Ding, Z. L., & Xiong, S. F. (2007). Magnetostratigraphy of the Neogene Sikouzi section at Guyuan, Ningxia, China. *Palaeogeography, Palaeoclimatology, Palaeoecology*, 243, 223–234. <https://doi.org/10.1016/j.palaeo.2006.07.016>
- Jin, X. C., Wang, J., Chen, B. W., & Ren, L. D. (2003). Cenozoic depositional sequences in the piedmont of the west Kunlun and their paleogeographic and tectonic implications. *Journal of Asian Earth Sciences*, 21, 755–765. [https://doi.org/10.1016/S1367-9120\(02\)00073-1](https://doi.org/10.1016/S1367-9120(02)00073-1)
- Li, X. Z., Dong, G. R., Chen, H. Z., Zheng, H. B., Jin, H. L., & Jin, T. (2001). Uplift processes of the Qinghai-Tibet plateau interpreted from the comparison of Yecheng section and Siwalik group. *Journal of Desert Research*, 21(4), 354–360.
- Lin, X. B., Chen, H. L., Wyrwoll, K. H., & Cheng, X. G. (2010). Commencing uplift of the Liupan Shan since 9.5 Ma: Evidences from the Sikouzi section at its east side. *Journal of Asian Earth Sciences*, 37, 350–360. <https://doi.org/10.1016/j.jseae.2009.09.005>
- Liu, D. L., Yan, M. D., Fang, X. M., Li, H. B., Song, C. H., & Dai, S. (2011). Magnetostratigraphy of sediments from the Yumu Shan, Hexi Corridor and its implications regarding the Late Cenozoic uplift of the NE Tibetan Plateau. *Quaternary International*, 236, 13–20. <https://doi.org/10.1016/j.quaint.2010.12.007>
- Liu, X. B., Shi, W., Hu, J. M., Fu, J. L., Yan, J. Y., & Sun, L. L. (2019). Magnetostratigraphy of Paleogene-Neogene sediments in the Yinchuan Basin and its implications for regional tectonics. *Journal of Asian Earth Sciences*, 173, 61–69.
- Peng, X. L. (1975). Location and horizon of Cenozoic vertebrate fossils in the Junggar Basin, Xinjiang. *Journal of Vertebrate Paleontology*, 13(3), 185–189.
- Qiao, L. L., Huang, B. C., Biggin, A. J., & Piper, J. D. A. (2017). Late Cenozoic evolution in the Pamir-Tian Shan convergence: New chronological constraints from the magnetostratigraphic record of the southwestern Tianshan foreland basin (Ulugqat area). *Tectonophysics*, 717, 51–64. <https://doi.org/10.1016/j.tecto.2017.07.013>
- Qiu, Z. X., & Ye, J. (1988). A new species of perocrocuta from Tongxin, Ningxia. *Vertebrata Palasiatica*, 26, 116–127.
- Region Geological Survey of Ningxia Hui Autonomous (RGSNX) (2000). *Regional geological survey report of Wuzhong (1:250,000)* (pp. 1–431). Beijing: Geological Publishing House.
- Sarikaya, A. M., Çiner, A., & Zreda, M. (2015). Fairy chimney erosion rates on Cappadocia ignimbrites, Turkey: Insights from cosmogenic nuclides. *Geomorphology*, 234, 182–191. <https://doi.org/10.1016/j.geomorph.2014.12.039>
- Sharma, P., Bourgeois, M., Elmore, D., Granger, D., Lipschutz, M. E., & Ma, X. (2000). PRIME lab AMS performance upgrades and research applications. *Nuclear Instruments Methods in Physics Research Section B: Beam Interactions with Materials and Atoms*, 172(1–4), 112–123. [https://doi.org/10.1016/S0168-583X\(00\)00132-4](https://doi.org/10.1016/S0168-583X(00)00132-4)
- Shen, X. H., Tian, Q. J., Ding, G. Y., Wei, K. B., & Chen, Z. W. (2001). The late Cenozoic stratigraphic sequence and its implication to tectonic evolution, Hejiakouzi area, Ningxia Hui Autonomous Region. *Earthquake Research China*, 17, 156–166.
- Shi, W., Chen, H., Li, Z. H., Gong, W. B., & Qiu, S. D. (2016). Regional geologic investigation methods in neotectonic and active tectonic area: Evidence from 1:50000 regional geologic mapping in neotectonic and active tectonic areas including Hongyazi, Dabazhan and Qingtongxialvchang in Ningxia. *Journal of Geomechanics*, 22(4), 856–867.
- Shi, W., Dong, S. W., Yuan, L., Hu, J. M., Chen, X. H., & Chen, P. (2015). Cenozoic tectonic evolution of the South Ningxia region, northeastern Tibetan Plateau inferred from new structural investigations and fault kinematic analyses. *Tectonophysics*, 649, 139–164. <https://doi.org/10.1016/j.tecto.2015.02.024>
- Shi, W., Liu, Y., Liu, Y., Chen, P., Chen, L., Cen, M., ... Li, H. Q. (2013). Cenozoic evolution of the Haiyuan fault zone in the northeast margin of the Tibetan Plateau. *Earth Science Frontiers*, 20, 1–17.
- Shi, X. H., Yang, Z., Dong, Y. P., Wang, S. D., He, D. F., & Zhou, B. (2018). Longitudinal profile of the Upper Weihe River: Evidence for the late Cenozoic uplift of the northeastern Tibetan Plateau. *Geological Journal*, 53(S1), 364–378. <https://doi.org/10.1002/gj.3195>
- Sun, J. M., Zhu, R. X., & Bowler, J. (2004). Timing of the Tianshan Mountains uplift constrained by magnetostratigraphic analysis of molasse deposits. *Earth and Planetary Science Letters*, 219, 239–253. [https://doi.org/10.1016/S0012-821X\(04\)00008-1](https://doi.org/10.1016/S0012-821X(04)00008-1)

- The Research Group on Active Fault System around Ordos Massif, State Seismological Bureau (RGAFSO) (1988). *Active fault system around Ordos massif* (pp. 1–335). Beijing: Seismological Press.
- Wang, B. Y., Yan, Z. Q., Lu, Y. J., & Chen, G. X. (1994). Discovery of two mid-Tertiary mammalian faunas from Haiyuan, Ningxia, China. *Vertebrata Palasiatica*, 32, 285–296.
- Wang, E., Wan, J. L., & Liu, J. Q. (2003). Late Cenozoic geological evolution of the foreland basin bordering the West Kunlun range in Pulu area: Constraints on timing of uplift of northern margin of the Tibetan Plateau. *Journal of Geophysical Research Solid Earth*, 108, 2401.
- Wang, W. T., Zhang, P. Z., & Kirby, E. (2011). A revised chronology for Tertiary sedimentation in the Sikouzi basin: Implications for the tectonic evolution of the northeastern corner of the Tibetan Plateau. *Tectonophysics*, 505, 100–114. <https://doi.org/10.1016/j.tecto.2011.04.006>
- Ye, Z., Gao, R., Li, Q. S., Zhang, H. S., Shen, X. Z., Liu, X. Z., & Gong, C. (2015). Seismic evidence for the North China plate underthrusting beneath northeastern Tibet and its implications for plateau growth. *Earth and Planetary Science Letters*, 426, 109–117. <https://doi.org/10.1016/j.epsl.2015.06.024>
- Zhang, K., & Cai, J. B. (2006). Preliminary result of the dating by TCN technique of the highest terrace of the heishanxia gorge mouth, northeast margin of Tibetan Plateau and its expression of neotectonic movement in that area. *Quaternary Sciences*, 26(1), 85–91.
- Zhang, P. Z., Burchfiel, B. C., Molnar, P., Zhang, W. Q., Jiao, D. C., Deng, Q. D., ... Song, F. M. (1990). Later Cenozoic tectonic evolution of the Ningxia-Hui Autonomous Region, China. *Geological Society of America Bulletin*, 102, 1484–1498.
- Zhang, P. Z., Burchfiel, B. C., Molnar, P., Zhang, W. Q., Jiao, D. C., Deng, Q. D., ... Song, F. M. (1991). Amount and style of late Cenozoic deformation in the Liupan Shan area, Ningxia Autonomous Region, China. *Tectonics*, 10, 1111–1129. <https://doi.org/10.1029/90TC02686>
- Zhang, Y. Q., Liao, C. Z., Shi, W., & Hu, B. (2006). Neotectonic evolution of the peripheral zones of the Ordos basin and geodynamic setting. *Geological Journal of China Universities*, 12, 285–297.
- Zhao, Z. J., Granger, D. E., Chen, Y., Shu, Q., Liu, G. F., Zhang, M. H., ... Qiao, L. L. (2017). Cosmogenic nuclide burial dating of an alluvial conglomerate sequence: An example from the Hexi Corridor, NE Tibetan Plateau. *Quaternary Geochronology*, 39, 68–78. <https://doi.org/10.1016/j.quageo.2017.02.007>

How to cite this article: Shi W, Hu J, Chen P, et al. Yumen conglomerate ages in the South Ningxia Basin, north-eastern Tibetan Plateau, as constrained by cosmogenic dating. *Geological Journal*. 2019;1–10. <https://doi.org/10.1002/gj.3510>